

# Polyhedral Decomposition of Hyperbolic 3-Manifolds with Totally Geodesic Boundary

Sadayoshi Kojima

*Dedicated to Professor Kunio Murasugi  
on his sixtieth birthday*

## §1. Introduction

A hyperbolic manifold will be a riemannian manifold with constant sectional curvature  $-1$ . It is shown by Epstein and Penner [1] that every noncompact complete hyperbolic manifold of finite volume, hence having cusps, is decomposed by ideal polyhedra. The decomposition supplies a quite convenient block to study several geometries of the cusped manifold especially in dimension three. See [4] for instance.

A variant of the construction by Epstein and Penner would establish a decomposition of a compact hyperbolic manifold with nonempty geodesic boundary by truncated polyhedra as well, which we plan to discuss in a forthcoming paper [3]. However the process will be rather unseen in the manifold.

In this paper, taking advantage of working only in dimension three, we give a more visible construction of this decomposition. In fact we directly show

**Theorem.** *Let  $N$  be a compact hyperbolic 3-manifold with non-empty totally geodesic boundary. Then the topological decomposition of  $N$  dual to the cut locus of  $\partial N$  modulo boundary is homotopic by straightening to a polyhedral decomposition.*

The visible process is expected to lead us to the deep understanding of geometry of those manifolds. We apply it for example to find the minimum of their volumes in [2].

We describe the rule of the decomposition in the next section with some detailed accounts of truncated polyhedra. We study the cut locus of the boundary and its topological dual decomposition in §3. Then we show in the subsequent sections that the straightening of the dual along its internal edges yields the final polyhedral decomposition. The proof of Proposition 5.2 thus finishes the proof of the theorem.

I am grateful to Tomoyoshi Yoshida for showing his idea to decompose cusped manifolds by ideal polyhedra.

## §2. Truncated polyhedra

We start with describing a basic piece of truncated polyhedra, called truncated tetrahedra. An ideal tetrahedron is a hyperbolic polyhedron identified with a finite volume region in the hyperbolic 3-space  $\mathbf{H}^3$  bounded by four geodesic planes, every two of which intersect each other, and every three of which intersect at infinity. An ultra ideal tetrahedron is one identified with a similar region bounded by four planes, every two of which intersect each other again but no three of which intersect even at infinity. If we are in the projective model, an ultra ideal tetrahedron is one whose vertices are located outside of the model disk.

An ultra ideal tetrahedron is of infinite volume. The truncation is the device to cut off its thick end by a geodesic plane which intersects three planes towards the end perpendicularly. Such truncation is always uniquely possible since

**Lemma 2.1.** *For any three metric disks on the euclidean plane which have no points in common but each two of which have a common region, there is a unique circle intersecting their boundaries perpendicularly.*

*Proof.* Let us name three disks by  $A$ ,  $B$  and  $C$ . By conformal change, we may assume that one of the intersection points of  $\partial A$  and  $\partial B$  is located at infinity. Then  $\partial A$  and  $\partial B$  are the lines intersecting say at the origin. By the assumption on the position of disks,  $C$  does not contain the origin. Hence we have a unique circle centered at the origin intersecting  $\partial C$  perpendicularly. This circle automatically intersects both  $\partial A$  and  $\partial B$  perpendicularly. Q.E.D.

Regard the boundaries of these disks as the ends of the geodesic planes which make up a thick end of an ultra ideal tetrahedron. The circle obtained in Lemma 2.1 will be the boundary of the plane for truncation. This plane intersects three planes perpendicularly. Cutting off each thick end by truncation, we get a compact polyhedron. This is a

truncated tetrahedron. The surface of a truncated tetrahedron consists of four right angle hexagons on the planes to bound the region, and four triangles produced by the truncation.

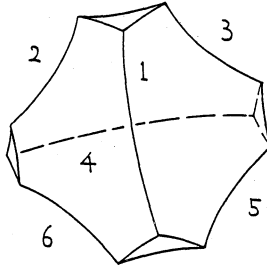


Fig. 1.

A convex truncated polyhedron can be described in a similar manner. Start with a finite set of geodesic planes in  $\mathbf{H}^3$ , no three of which intersect even at infinity. Assume that it bounds a noncompact convex region each thick end of which admits truncation. Then cutting off each end of the region by truncation, we get a compact polyhedron. This is a convex truncated polyhedron. The surface of a convex truncated polyhedron consists of right angle polygons on the planes, which we call internal faces, and the other polygons produced by the truncation, which we call external faces. The union of internal faces is connected, while external faces are mutually disjoint.

A tetrahedron is a basic piece of a polyhedron even in this situation.

**Lemma 2.2.** *A convex truncated polyhedron is decomposed by truncated tetrahedra without producing vertices in the interior.*

*Proof.* Choose an external face  $\tau$  and introduce the shortest geodesic paths from the face to the other external faces. Such a path uniquely exists for each face. It lies on the boundary if  $\tau$  and the terminal face are joined by just one face. Obviously it lies on this joining face then. Otherwise the paths go through interior of the polyhedron.

The internal faces touching  $\tau$  are now subdivided into right angle hexagons. Subdivide then the other internal faces by a geodesic path into right angle hexagons arbitrarily. Each geodesic path introduced

here joins two external faces. It together with the shortest paths assigned to the terminal faces span a right angle hexagon in the interior of the polyhedron. Because two paths determine a geodesic plane intersecting three external faces involved perpendicularly and hence this plane must contain the last path. The collection of these hexagons divides the original polyhedron into truncated tetrahedra. Q.E.D.

A *polyhedral decomposition* of a hyperbolic 3-manifold with totally geodesic boundary is a geometric cellular decomposition by (convex) truncated polyhedra so that their external faces form the boundary. This justifies our naming for faces. We also call an edge internal if it is an intersection of two internal faces, and external otherwise. Notice in this decomposition that every internal edge is a geodesic path from the boundary to the boundary.

Let us describe a parametrization of isometry classes of labelled truncated tetrahedra to show its variation, though the result is not needed for the proof of the theorem. The isometry class of a truncated tetrahedron is determined by the mutual position of the internal faces, since the truncation is unique. Label the internal edges as in Figure 1.1 and denote the dihedral angle along the edge  $j$  by  $\theta_j$ .  $\theta_j$ 's are quantities to describe mutual position. The sum of three dihedral angles having a common external face must be less than  $\pi$  because otherwise three planes towards the end meet in the real world. Thus we have a necessary condition,

$$\left\{ \begin{array}{l} \theta_1 + \theta_2 + \theta_3 < \pi \\ \theta_1 + \theta_5 + \theta_6 < \pi \\ \theta_2 + \theta_4 + \theta_6 < \pi \\ \theta_3 + \theta_4 + \theta_5 < \pi. \end{array} \right.$$

Conversely,

**Lemma 2.3.** *For  $\theta_1, \dots, \theta_6$  satisfying the above inequalities, there is a unique labelled truncated tetrahedron with these dihedral angles.*

*Proof.* Make four geodesic triangles using  $\theta_1, \dots, \theta_6$  which would form external faces. They have twelve edge lengths as data we can use. Choose a triple from these twelve lengths that would be assigned to the external edges of an internal face we expect to make. Then there is a unique right angle hexagon having these as non adjacent edge lengths, which is a candidate of the internal face. Applying the same for the other triples, we get four right angle hexagons.

The expected truncated tetrahedra should be obtained by gluing these faces in  $\mathbf{H}^3$ , and what we need to show now is that the length of a common internal edge for each pair of hexagons made are the same. We do this for the internal edge 1. By the hyperbolic cosine rule, we have

$$(*) \quad \cosh l_{ij} = \frac{\cos \theta_i \cos \theta_j + \cos \theta_k}{\sin \theta_i \sin \theta_j},$$

where  $\{i, j, k\}$  corresponds to 3 angles of a triangle and  $l_{ij}$  is the length of the external edge connecting edges  $i$  and  $j$ . We made two hexagons having the edge 1. By the hexagon rule [4], the length  $l_1$  of the edge 1 computed in the hexagon having the edges 2 and 6 is given by

$$\cosh l_1 = \frac{\cosh l_{12} \cosh l_{16} + \cosh l_{26}}{\sinh l_{12} \sinh l_{16}},$$

and the same having the edges 3 and 5 is given by

$$\cosh l_1 = \frac{\cosh l_{13} \cosh l_{15} + \cosh l_{35}}{\sinh l_{13} \sinh l_{15}}.$$

It is then easy to check by substitution of (\*) that right hand sides of both identities are the same. Q.E.D.

### §3. Cut locus

Studying several properties of the cut locus of the boundary in this section, we will find a topological cellular decomposition of a hyperbolic manifold with totally geodesic boundary. It is dual to the cut locus modulo boundary and turns out to be equivalent to the final one. The decomposition will be denoted by  $K$ .

Here we start with making a few conventions used throughout the sequel. Let  $N$  be a compact hyperbolic 3-manifold with totally geodesic boundary  $\partial N$ . Let  $\pi : \tilde{N} \rightarrow N$  be the universal covering of  $N$ . We use the symbol  $\tilde{X}$  to denote the preimage of a subspace  $X$  of  $N$  in  $\tilde{N}$ . We always identify the universal cover  $\tilde{N}$  with a subspace in  $\mathbf{H}^3$ . Then the boundary  $\partial \tilde{N}$  of the universal cover  $\tilde{N}$  or the preimage  $\widetilde{\partial N}$  of the boundary  $\partial N$  is formed by geodesic planes in  $\mathbf{H}^3$ . We often identify a cell complex with its underlying polyhedron. The symbol  $Y^{(k)}$  will be used to denote the  $k$ -skeleton of a cell complex  $Y$  as usual.

We define three terminologies for our convenience. To each pair of components of  $\partial \tilde{N}$ , associated is a unique shortest path connecting them. We call this path a *short cut*. Also there is an associated bisectorial

geodesic plane to the short cut in  $\mathbf{H}^3$ . We call this plane a *middle fence*. A short cut descends to the geodesic path in  $N$  from the boundary to the boundary. We call such a path a *return path*. Though it may come back to a different component, we wish to emphasize by this name that it comes back to the boundary anyway. These are the terminologies we shall use frequently.

The cut locus  $\mathbf{C}$  of  $\partial N$  in  $N$  is a subset in  $\text{int } N$  which consists of the points that admit at least two distinct shortest paths to  $\partial N$ . Obviously a point on  $\mathbf{C}$  lifts to a point on the middle fence of some short cut.  $\mathbf{C}$  is canonically stratified by grouping the points which have the same number of shortest paths to the boundary. This stratification is quite nice in our case since

**Proposition 3.1.** *The stratification defines a convex cellular decomposition of the cut locus  $\mathbf{C}$ .*

A point on  $\mathbf{C}$  is in a 2-cell if it admits precisely two shortest paths to the boundary, however the number of shortest paths the point admits is rather unrelated with the dimension of the cell in the other case. To see this proposition, we need a few preliminaries.

**Lemma 3.2.** *Suppose that  $A$  and  $B$  are ultra parallel planes of distance  $d$  in  $\mathbf{H}^3$ . Then the orthogonally projected image of  $A$  to  $B$  is an open metric disk of radius  $\text{arccosh}(\coth d)$ .*

*Proof.* This is an easy consequence of length calculus for a hyperbolic rectangle with one ideal vertex and three vertices of right angle as in Figure 2.

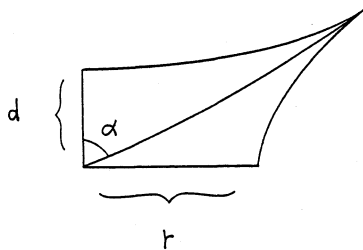


Fig. 2.

The hyperbolic cosine rule shows the identities;

$$\cosh d = \frac{1}{\sin \alpha},$$

$$\cosh r = \frac{1}{\sin(\pi/2 - \alpha)} = \frac{1}{\cos \alpha}.$$

Then we are done by solving the relation between  $d$  and  $r$  in terms of  $r$ . Q.E.D.

**Corollary 3.3.** *There exist only finitely many return paths with bounded length.*

*Proof.* Choose a component  $S$  of  $\partial\tilde{N}$ , and project the other boundary components orthogonally to  $S$ . Then we get an open disk packing on  $S$  invariant under the action of the covering transformations preserving  $S$ . Hence  $\pi(S) \subset N$  is packed by open balls. It is obvious by definition that the packing on  $\pi(S)$  does not depend on the choice of a component  $S$  of  $\pi^{-1}(\pi(S))$ . Applying the same process to all the other components, we get a ball packing on  $\partial N$ . The radius of each ball is related to the length of the associated return path by Lemma 3.2. Since  $\partial N$  is compact, the number of balls packing  $\partial N$  with bounded radius away from zero is obviously finite. Hence there are only finitely many return paths of bounded length. Q.E.D.

*Proof of Proposition 3.1.* Choose a component  $U$  of the complement of  $\tilde{\mathbf{C}}$  in  $\tilde{N}$  and let  $S$  be its boundary in  $\partial\tilde{N}$ .  $U$  is invariant under the action of covering transformations preserving  $S$ . We are interested in the internal boundary of the closure  $\bar{U}$  of  $U$  not meeting  $\partial\tilde{N}$ . It is a part of  $\tilde{\mathbf{C}}$  and formed by a part of middle fences. Since  $N$  is compact, its diameter is bounded, and the points on  $\mathbf{C}$  have bounded distance to  $\partial N$ . The shortest arc from a point on  $\mathbf{C}$  to  $\partial N$  is lifted to an arc in  $\bar{Y}$ . In particular, the distance between  $S$  and any point on the internal boundary of  $\bar{U}$  is bounded. Hence the middle fences involved in this boundary are associated with the short cuts of bounded length.

By Corollary 2.3, there are only finitely many return paths with bounded length. Hence the middle fences involved in the internal boundary of  $\bar{U}$  belong to only finitely many orbits of middle fences by the action of covering transformations preserving  $S$ . The internal boundary of  $\bar{U}$  thus gets a locally finite invariant cellular decomposition induced by the intersection of middle fences involved. It descends to a cellular decomposition of the internal boundary of  $\pi(\bar{U})$ .

We can apply the same argument to the other component. It is an exercise to check that the cell structures for the common part of different internal boundaries are identical. Hence we get an invariant cellular decomposition of  $\tilde{\mathbf{C}}$  and hence a cell complex structure of  $\mathbf{C}$ . Each 2-cell of  $\mathbf{C}$  is convex since it lifts to a convex polygon on some middle fence bounded by the intersections with a finite number of the other middle fences. Q.E.D.

From now on, let us mean by  $\mathbf{C}$  not only the cut locus itself but endowed with this cellular decomposition by virtue of the proposition. In the universal cover, we say a 2-cell of  $\tilde{\mathbf{C}}$  faces a component of  $\partial\tilde{N}$  if the cell can be projected orthogonally to the component by the shortest paths to  $\partial\tilde{N}$ . Each 2-cell faces two boundary components associated to the middle fence containing it. The set of orthogonal projections for each 2-cell to these components gives rise to an equivariant one-to-finite orthogonal projection:  $\tilde{\mathbf{C}} \rightarrow \partial\tilde{N}$ . The number of the image of  $p \in \tilde{\mathbf{C}}$  is equal to the number of the shortest paths from  $p$  to  $\partial\tilde{N}$ . The cellular decomposition of  $\tilde{\mathbf{C}}$  is conveyed to an invariant convex polygonal decomposition of  $\partial\tilde{N}$ . In particular, the cellular decomposition of  $\mathbf{C}$  induces a convex polygonal decomposition of  $\partial N$ .

Now, we would like to build up a topological cellular decomposition  $K$  of  $N$  dual to  $\mathbf{C}$  modulo boundary. Start with defining a compact 3-cell, which we call a block, in the universal cover. Its interior will be a 3-cell in the precise definition of the cell complex  $K$ . Take an invariant graph  $G$  on  $\tilde{\mathbf{C}}$  under the action of  $\pi_1(N)$  which is dual to the 1-skeleton  $\tilde{\mathbf{C}}^{(1)}$ . Here we mean by dual, the 1-dimensional subcomplex of the barycentric like subdivision of  $\tilde{\mathbf{C}}$  spanned by vertices not in  $\tilde{\mathbf{C}}^{(0)}$ . Then project it by the one-to-finite orthogonal projection to  $\partial\tilde{N}$ . The trace of the projection determines a fence which divides  $\tilde{N}$  into equivariant pieces homeomorphic to a ball. This is a block to built up  $\tilde{K}$ .

Let us next define a compact cell which we call a face, an edge or a vertex according to its dimension. The intersection of two blocks is the trace of the star subgraph of a vertex of  $G$  on a 1-cell of  $\tilde{\mathbf{C}}$  by the orthogonal projection. Hence take it as a dual face to the 1-cell of  $\tilde{\mathbf{C}}$  on which the center is located, and call it an internal face. We also take a component of the intersection of a block and  $\partial\tilde{N}$  as an external face. A face will be either an internal or external face. The intersection of two internal faces is the trace of a vertex of  $G$  on a 2-cell of  $\tilde{\mathbf{C}}$ . Hence take it as a dual edge to the 2-cell containing the vertex, and call it an internal edge. We also take a component of the intersection of an

internal face and  $\partial\tilde{N}$  as an external edge. An edge will be either an internal or external edge. Finally a vertex will be a terminal point of an edge.

Then let  $\tilde{K}$  be a cellular decomposition of  $\tilde{N}$  by the interior of blocks, faces, edges and vertices. Since it is invariant under the action of  $\pi_1(N)$ , it determines a cellular decomposition  $K = \pi(\tilde{K})$  of  $N$ . This is what we call a dual to  $\mathbf{C}$  modulo boundary. Notice that  $\partial K$  is dual to the convex polygonal decomposition of  $\partial N$  induced by the cut locus.

We describe the compact cells of  $\tilde{K}$  more locally to visualize the situation. Each block contains a unique 0-cell of  $\tilde{\mathbf{C}}$ . We call this a center. Choose a block  $\sigma$  with the center  $p$  and let us describe its combinatorial structure of the boundary by identifying  $p$  with the origin of the 3-dimensional Poincaré disk.  $p$  has the shortest rays to finitely many components of  $\partial\tilde{N}$ , say  $S_1, S_2, \dots, S_m$ .  $\sigma$  can be identified with a regular neighborhood of the union of these rays. The ray extends and terminates in the sphere at infinity  $S_\infty^2$ . The terminal point  $q_j$  is the center of the metric circle  $\partial S_j$  on  $S_\infty^2$  with respect to the canonical spherical metric, where  $j = 1, 2, \dots, m$ . Notice that the radii of circles are the same because the distances from the origin are the same.

Take the cut locus  $\mathbf{D}$  of the point set  $\{q_1, \dots, q_m\}$  on  $S_\infty^2$ .  $\mathbf{D}$  consists of the points on  $S_\infty^2$  which admit at least two shortest paths to the set  $\{q_1, \dots, q_m\}$ .  $\mathbf{D}$  is unit tangentially equivalent to  $\mathbf{C}$  at  $p$  and hence determines a convex polygonal decomposition on  $S_\infty^2$ .

A topological dual decomposition  $\mathbf{D}^*$  of  $\mathbf{D}$  on  $S_\infty^2$  with vertices  $q_1, \dots, q_m$  is identified with one obtained from the cellular decomposition of  $\partial\sigma$  by collapsing each external face to  $q_j$ . Notice by the definition of the cut locus that the vertices of a face of  $\mathbf{D}^*$  have the same distance to the vertex of  $\mathbf{D}$  in this face. This fact will be used later.

We may assume that each edge of  $\mathbf{D}^*$  is straight at least in the disks bounded by  $\partial S_j$ 's. Replacing the part of  $\mathbf{D}^*$  in each disk by  $\partial S_j$ , we get a cellular decomposition  $\mathbf{D}^{**}$  on  $S_\infty^2$ .  $\mathbf{D}^{**}$  is equivalent to  $\partial\sigma$ .

There are several immediate correspondence by the identification of  $\partial\sigma$  and  $\mathbf{D}^{**}$ . The external faces correspond to the faces bounded by  $\partial S_j$ 's, and the internal faces do to the others. The external edges correspond to the edges on  $\partial S_j$ 's, while the internal edges do to the others. The vertices on the circle  $\partial S_j$  correspond to 2-cells of  $\mathbf{C}$  which touches  $p$  and faces  $S_j$ . Both are arranged in the same order.

The final decomposition is obtained by straightening each edges of  $\tilde{K}$ . The straightening here is the device first to replace each internal edges by homotopic short cuts, and then to replace external edges by geodesic paths using their end points. The straight map we get is sup-

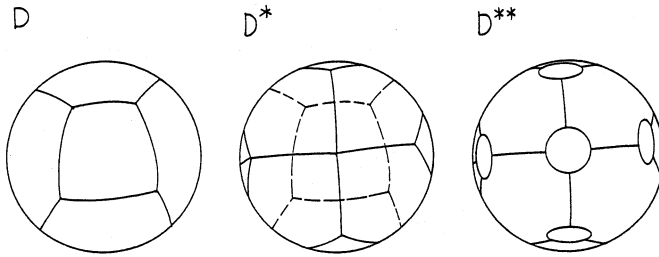


Fig. 3.

ported on the 1-skeleton  $K^{(1)}$  at the beginning and there is no obvious reasons why it creates something good. The rest of this paper is to check the reason why it does.

The first step is to observe that the image of  $\partial K^{(1)}$  by the straight map, which will be denoted by  $\partial\Delta^{(1)}$ , turns out to be a 1-skeleton of a convex polygonal decomposition of  $\partial N$ , denoted by  $\partial\Delta$ . This will be done in the next section. The second step starts by showing that the map can be straightened over the 2-skeleton  $K^{(2)}$ . The main step is then to observe that the straightened image of  $K^{(2)}$ , denoted by  $\Delta^{(2)}$ , turns out to be a 2-skeleton of a convex polyhedral decomposition of  $N$ , denoted by  $\Delta$ . Since we define the final decomposition  $\Delta$  from the lower dimensional skeletons, the accessories for  $\Delta$  we use is not appropriate in fact, but will be justified by the end of the paper.

#### §4. Polygonal decomposition

We study the effect of straightening on the boundary in this section, and prove that the straightening defines a convex polygonal decomposition of  $\partial N$  equivalent to  $\partial K$ . The argument will be given mainly in the universal cover.

An internal edge of  $\tilde{K}$  bridges two components of  $\partial\tilde{N}$ . Hence to each internal edge, assigned is a unique middle fence and a unique short cut. Recall that an internal edge is a dual to a 2-cell of  $\tilde{C}$  which lies on this middle fence. The number of orbits of short cuts associated to 2-cells of  $\tilde{C}$  by the action of  $\pi_1(N)$  was finite. Let  $\tilde{\mathbf{R}}$  be the set of these short cuts, and  $\mathbf{R} = \pi(\tilde{\mathbf{R}})$  be the set of descending return paths in  $N$ .  $\mathbf{R}$  is a finite set.

The straightening device at this stage is precisely to connect vertices of  $\tilde{\mathbf{R}}$  by geodesic paths if the corresponding two vertices in  $\partial\tilde{K}^{(0)}$  are joined by an external edge. We denote the resultant geodesic 1-complex by  $\partial\tilde{\Delta}^{(1)}$  in the abstract sense. The accessories in the notation should be ignored for the moment. The definition does not immediately tell us that  $\partial\tilde{\Delta}^{(1)}$  is an embedded 1-complex. What we obviously know by definition is that  $\partial\tilde{\Delta}^{(1)}$  is invariant under the action of  $\pi_1(N)$ , and that there is an equivariant graph isomorphism  $h : \partial\tilde{K}^{(1)} \rightarrow \partial\tilde{\Delta}^{(1)}$ .

Since the connection rule to build up  $\partial\tilde{\Delta}^{(1)}$  was followed by the rule for  $\partial\tilde{K}^{(1)}$ ,  $\partial\tilde{\Delta}^{(1)}$  should be very similar to  $\partial\tilde{K}^{(1)}$ . The claim to be proved is that  $\partial\tilde{\Delta}^{(1)}$  is in fact a 1-skeleton of an invariant convex polygonal decomposition  $\partial\tilde{\Delta}$  of  $\partial\tilde{N}$ , and  $h$  extends to an equivariant cellular isomorphism of  $\partial\tilde{K}$ . The statement in  $\partial N$  is hence

**Proposition 4.1.**  $\partial\Delta^{(1)} = \pi(\partial\tilde{\Delta}^{(1)})$  turns out to be a 1-skeleton of a convex polygonal decomposition  $\partial\Delta = \pi(\partial\tilde{\Delta})$  of  $\partial N$  equivalent to  $\partial K$ .

To see this, we need a few observations about local structure of edges in  $\partial\tilde{\Delta}^{(1)}$ . The first one is about the image of the boundary of a face of  $\partial\tilde{K}$ .

**Lemma 4.2.** *The image of the boundary of a face of  $\partial\tilde{K}$  by  $h$  bounds a convex polygon on  $S$ . The canonical extension of  $h$  to the face preserves the orientation.*

*Proof.* Choose a face  $\tau$  of  $\partial\tilde{K}$  and assume that it lies on a block  $\sigma$  with the center  $p$ . The cellular decomposition of  $\partial\sigma$  was described by  $\mathbf{D}^{**}$ . The external face  $\tau$  is identified with a face bounded by a metric circle  $\partial S$  on  $S_\infty^2$ . The center  $q$  of  $\partial S$  is the terminal point of an extension of the shortest path from  $p$  to  $S$ .

Label the vertices of  $\tau$  by  $v_j$  with  $j = 0, 1, \dots, n - 1$  in counter-clockwise order. Each vertex is a projected image of a dual vertex to a 2-cell in  $\tilde{\mathbf{C}}$  touching  $p$  and facing  $S$ . Hence we also label the 2-cell of  $\tilde{\mathbf{C}}$  corresponding to  $v_j$  by  $F_j$ .

Each  $F_j$  is on the middle fence of a short cut from a point on  $S$  since  $F_j$  faces  $S$ . Hence we let its starting point on  $S$  by  $w_j$ . Because of the definition of labeling, any adjacent  $w_j$ 's are joined by an edge in  $\partial\tilde{\Delta}^{(1)}$ .  $h(\partial\tau)$  is then a 1-complex formed by geodesic paths  $w_j w_{j+1}$  with  $j = 0, 1, \dots, n - 1$ , where  $j$  counts modulo  $n$  as usual.

We show that the vertices  $w_{j_0}, w_{j_1}, w_{j_2}$  span a triangle  $\Delta w_{j_0} w_{j_1} w_{j_2}$ , and its orientation assigned by how the vertices round induces the counterclockwise orientation on  $S$  as long as  $j_0 < j_1 < j_2$  up to cyclic permutation. Then using this property, we will get the conclusion by contradiction.

Identify  $S$  with the 2-dimensional Poincaré disk and  $q$  with the origin. The middle fences containing  $F_{j_0}, F_{j_1}, F_{j_2}$  respectively are orthogonally projected to three open metric disks  $B_{j_0}, B_{j_1}, B_{j_2}$  on  $S$  including the origin. The vertices  $w_{j_0}, w_{j_1}, w_{j_2}$  are the centers of these disks. The outside of  $\partial S$  is reflected into the inside by the orthogonal projection to  $S$ . The picture of the projection is shown in Figure 4.

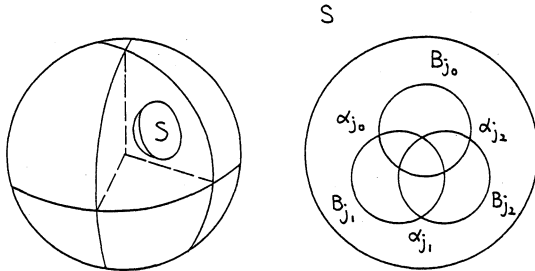


Fig. 4.

By the convexity of  $\mathbf{D}$ ,  $B_{j_0}, B_{j_1}$  and  $B_{j_2}$  are arranged in counterclockwise order as in the second picture in Figure 4. We named the intersections of the boundary of balls as in the figure. Then  $\alpha_{j_0}, \alpha_{j_1}$ , and  $\alpha_{j_2}$  determine the oriented triangle  $\Delta \alpha_{j_0} \alpha_{j_1} \alpha_{j_2}$  inducing the counterclockwise orientation on  $S$ .

Here is an elementary geometry. Let  $\gamma_{j_0}, \gamma_{j_1}, \gamma_{j_2}$  be the bisectors to the segments  $\alpha_{j_2} \alpha_{j_0}, \alpha_{j_0} \alpha_{j_1}$  and  $\alpha_{j_1} \alpha_{j_2}$  on  $S$  respectively. These three lines meet at the center  $\beta$  of the circumscribed circle of the triangle  $\Delta \alpha_{j_0} \alpha_{j_1} \alpha_{j_2}$ .  $w_j$  is on  $\gamma_j$ , where  $j = j_0, j_1, j_2$ . Since  $B_{j_0}, B_{j_1}, B_{j_2}$  do not contain  $\alpha_{j_1}, \alpha_{j_2}, \alpha_{j_0}$  respectively, the direction of the vector  $\beta w_j$  is the same as that of the outward vector from the triangle  $\Delta \alpha_{j_0} \alpha_{j_1} \alpha_{j_2}$  along  $\gamma_j$ . Hence the centers  $w_{j_0}, w_{j_1}, w_{j_2}$  are arranged in counterclockwise order from the viewpoint  $\beta$ , and determines an oriented triangle  $\Delta w_{j_0} w_{j_1} w_{j_2}$  inducing the counterclockwise orientation on  $S$ .

Suppose now that the union of geodesic paths  $w_j w_{j+1}$  with  $j =$

$0, \dots, n - 1$  does not bound a convex polygon on  $S$ . Then since any three vertices determines a nondegenerate triangle, there are suffices  $0 \leq j_3, j_4 \leq n - 1$  so that  $w_{j_3} w_{j_3+1}$  meets the biinfinite extension of  $w_{j_4} w_{j_4+1}$  at an interior point. Then the induced orientations on  $S$  by the triangles  $\Delta w_{j_3} w_{j_4} w_{j_4+1}$  and  $\Delta w_{j_3+1} w_{j_4} w_{j_4+1}$  are different each other. This contradicts what we have proved.

Since the vertices  $v_j$ 's of  $\tau$  and the corresponding vertices  $w_j$ 's of the convex polygon mapped by  $h$  are both arranged in counterclockwise order, a canonical extension of  $h$  preserves the orientation. Q.E.D.

We need one more observation about the structure around the vertex of  $\partial\tilde{K}$ . Label all the edges coming to the vertex of  $\partial\tilde{K}$ . Then by the connection rule of  $\partial\tilde{\Delta}^{(1)}$ , this labeling is canonically conveyed to the labeling of the edges of  $\partial\tilde{\Delta}^{(1)}$  which terminate at the corresponding vertex.

**Lemma 4.3.** *The counterclockwise orders of the labeling at a vertex of  $\partial\tilde{K}^{(1)}$  and the corresponding vertex of  $\partial\tilde{\Delta}^{(1)}$  are the same up to cyclic permutation.*

*Proof.* Choose a vertex  $v$  of  $\partial\tilde{K}$  and assume that it lies on a block  $\sigma$ . The cellular decomposition of  $\partial\sigma$  is described by  $\mathbf{D}^{**}$ .  $v$  is identified with a vertex on the metric circle  $\partial S$ .

Choose an adjacent vertex  $v'$  to  $v$  on the same circle  $\partial S$ .  $v$  and  $v'$  correspond to 2-cells  $F$  and  $F'$  in  $\tilde{\mathbf{C}}$  facing  $S$  and touching the center of  $\sigma$ . Recall that the adjacency is reflected by the property that these 2-cells  $F$  and  $F'$  have a common 1-cell. Denote by  $w$  and  $w'$  the vertices of  $\partial\tilde{\mathbf{R}}$  corresponding to  $v$  and  $v'$  respectively. Here is a geometric relation between the adjacency of  $v, v'$  and  $w, w'$ . The middle fence  $L$  containing  $F$  has an intersection line  $l$  with the middle fence  $L'$  containing  $F'$ .  $F$  is orthogonally projected to a convex polygon  $P$  on  $S$  and  $l$  is to a geodesic  $l_S$  which is an biinfinite extension of an edge of  $P$ . The plane determined by short cuts from  $w$  and  $w'$  is orthogonal to both  $L$  and  $L'$ , and in particular to  $l$ . Hence the geodesic path connecting  $w$  and  $w'$  extends to a biinfinite path  $\omega$  orthogonal to  $l_S$ .

What we have seen is that to each pair of  $v$  and  $v'$ , and hence to each edge coming to  $v$ , associated is an biinfinite extension  $l_S$  of an edge of  $P$ , and that  $w'$  lies on the geodesic  $\omega$  through  $w$  and orthogonal to  $l_S$ . Furthermore, though the vertices  $w$  and  $w'$  may not be separated by  $l_S$ , the vector from  $w$  to  $w'$  is directed towards the component of  $S - l_S$  not containing  $P$ , as the vector from  $v$  to  $v'$  obviously is.

Now identify  $S$  with the 2-dimensional Poincaré disk. The biinfinite

extensions of the edges of  $P$  determine a line configuration on  $S$ . Each line inherits a label from the associated edge coming to  $v$ . To each labelled line, we assign the orthogonal ray from  $v$  endowed with the same label. The counterclockwise order of the labeling for orthogonal rays is the same as that for edges of  $\partial\tilde{K}$  coming to  $v$ .

Then for each point on  $S$ , draw orthogonal rays to the geodesic lines again keeping the outward direction from  $P$ . Then the assignment of the counterclockwise order of the labeling of rays is a continuous function on  $S$  to the set of cyclic orders possibly with singularities. The singularity occurs only if two rays coincide. This may happen when two geodesic lines are ultra parallel. However in this case, the direction of associated two rays must be opposite since the region bounded by such lines contains a convex polygon  $P$ . Hence this continuous function has no singularities with discrete image. In particular, the order at  $w$  is the same as one at  $v$ . Q.E.D.

*Proof of Proposition 4.1.* By Lemma 4.2, extending a graph isomorphism  $h : \partial\tilde{K}^{(1)} \rightarrow \partial\tilde{\Delta}^{(1)}$ , we get a map  $h$  (still using the same notation) of  $\partial\tilde{K}$  by assigning to each face of  $\partial\tilde{K}$  a polygon bounded by corresponding edges of  $\partial\tilde{\Delta}^{(1)}$ . Here  $h$  is a local homeomorphism on the interior of faces. Since  $h$  preserves the orientation for each face, it must be a homeomorphism also around edges. Lemma 4.3 shows that the corners of convex polygons fill up a neighborhood of the vertices. Hence  $h$  is a local homeomorphism also around the vertices. It is easy to see that  $h$  is surjective. Since the image is simply connected,  $h$  is a global homeomorphism.

$\partial\tilde{\Delta}^{(1)}$  now determines a convex polygonal decomposition  $\partial\tilde{\Delta}$  of  $\partial\tilde{N}$ . The decomposition is invariant under the action of  $\pi_1(N)$ , and the map  $h$  can be chosen to be equivariant. Hence it determines a convex polygonal decomposition  $\partial\Delta = \pi(\partial\tilde{\Delta})$  of  $\partial N$  with a descending equivalence from  $\partial K$  to  $\partial\Delta$ . Q.E.D.

## §5. Polyhedral decomposition

In this section, we study the effect of straightening in the interior and finish to prove that the straightening determines a convex polyhedral decomposition of  $N$ , which we promised to denote by  $\Delta$ . The argument will be given again mainly in the universal cover.

The map  $h : \partial\tilde{K}^{(1)} \rightarrow \partial\tilde{\Delta}^{(1)} \subset \partial\tilde{N}$  we had at the beginning was a graph isomorphism. The main claim in §4 was that  $h$  extends to a cellular map  $h$  on  $\partial\tilde{K}$  to  $\partial\tilde{\Delta}$ . It obviously further extends as a cellular

isomorphism to  $h : \partial\tilde{K} \cup \tilde{K}^{(1)} \rightarrow \partial\tilde{\Delta} \cup \tilde{\mathbf{R}} \subset \tilde{N}$ . We then will see first that the map  $h$  extends as a straight map over the 2-skeleton  $\tilde{K}^{(2)}$ , showing that the image of the boundary of each internal face of  $\tilde{K}$  spans a geodesic polygon. Namely,  $\partial\tilde{\Delta} \cup \tilde{\mathbf{R}}$  extends to a geodesic 2-complex  $\tilde{\Delta}^{(2)}$  in  $\tilde{N}$  in the abstract sense.

**Lemma 5.1.** *The image of the boundary of an internal face of  $\tilde{K}$  by  $h$  bounds a right angle polygon on a geodesic plane in  $\tilde{N}$ .*

*Proof.* Choose an internal face  $\tau$  and assume that it lies on a block  $\sigma$ . The cell decomposition of  $\partial\sigma$  was described in  $\mathbf{D}^{**}$  by identifying the center  $p$  of  $\sigma$  with the origin of the 3-dimensional Poincaré disk. There are metric circles  $\partial S_1, \dots, \partial S_m$  on  $S_\infty^2$  which are the boundaries of the nearest components of  $\partial\tilde{N}$  from  $p$ . The centers  $q_1, \dots, q_m$  of these metric circles are also the endpoints of the rays extending the shortest path from the origin to the component  $S_j$ . The circles  $\partial S_1, \dots, \partial S_m$ , having the same radius, lie in the complement of the cut locus  $\mathbf{D}$  of  $\{q_1, \dots, q_m\}$  on  $S_\infty^2$ .

The face  $\tau$  is identified with a face not bounded by  $\partial S_j$ 's. We rearrange  $\partial S_j$ 's so that  $\partial\tau$  passes through  $\partial S_1, \partial S_2, \dots, \partial S_k$  in counterclockwise order.  $\tau$  contains a vertex  $u$  of a cut locus  $\mathbf{D}$ . Recall as we noted in the description of  $\mathbf{D}$  and  $\mathbf{D}^*$  that every  $\partial S_j$  has the same distance from  $u$ . In particular, there is a circle  $\partial H$  on  $S_\infty^2$ , bounding a geodesic plane  $H$  in the 3-dimensional Poincaré disk, that intersects orthogonally to each  $\partial S_1, \dots, \partial S_k$  simultaneously. Moreover,  $\partial H$  passes through  $\partial S_1, \dots, \partial S_k$  in counterclockwise order also.

$h(\partial\tau)$  is a piecewise geodesic whose bent occurs only at the end of external and hence internal edges. Each internal edge is mapped to the short cut between  $S_j$  and  $S_{j+1}$ . It must lie on the plane  $H$  since it intersects both  $S_j$  and  $S_{j+1}$  orthogonally. In particular, the image of internal edges is on a geodesic plane  $H$ . The image of external edges is on  $S_j$ 's and on  $H$  since the intersection of  $S_j$  and  $H$  is a geodesic passing two end points of the short cuts. It is then obvious by the order of intersections to  $\partial S_j$ 's that  $h(\partial\tau)$  bounds a convex polygon on  $H$ .

Q.E.D.

Denote by  $\tilde{\Delta}^{(2)}$  the collection of the straight image of each internal faces by Lemma 5.1 and  $\partial\tilde{\Delta} \cup \tilde{\mathbf{R}}$ . The accessories in this notation should be ignored for the moment. The definition does not immediately tell us that  $\tilde{\Delta}^{(2)}$  is an embedded 2-complex. What we obviously know by definition is that  $\tilde{\Delta}^{(2)}$  is invariant under the action of  $\pi_1(N)$ , and that

there is an equivariant cellular isomorphism  $h : \tilde{K}^{(2)} \rightarrow \tilde{\Delta}^{(2)}$  which extends the original  $h$ . The claim to be proved is that  $\tilde{\Delta}^{(2)}$  is in fact a 2-skeleton of an invariant convex polyhedral decomposition  $\tilde{\Delta}$  of  $\tilde{N}$ , and  $h$  extends to an equivariant cellular isomorphism of  $\tilde{K}$ . The statement in  $N$  is our final goal.

**Proposition 5.2.**  $\Delta^{(2)} = \pi(\tilde{\Delta}^{(2)})$  turns out to be a 2-skeleton of a convex polyhedral decomposition  $\Delta = \pi(\tilde{\Delta})$  of  $N$  equivalent to  $K$ .

We have shown so far that if we restrict the map  $h$  to the set of external faces or to each internal face, then  $h$  is an embedding. What we still do not know is if the image of some internal faces intersect. To see our final proposition, we proceed further to a local study.

**Lemma 5.3.** *The image of the boundary of a block of  $\tilde{K}$  by  $h$  bounds a convex polyhedron in  $\tilde{N}$ .*

*Proof.* Choose a block  $\sigma$  and recall that the cell decomposition of  $\partial\sigma$  is described by  $\mathbf{D}^{**}$  on  $S_\infty^2$ . Assigned to each external face was a geodesic boundary  $S_j$ , and assigned to each internal face  $\tau_i$  now by Lemma 5.1 is a geodesic plane  $H_i$  in  $\mathbf{H}^3$ . Using this description, we will define a continuous deformation  $\{h_t\}$  of a restriction of  $h$  to  $\partial\sigma$ ,  $h|_{\partial\sigma} = h_0$ , so that it eventually pushes the image of internal faces out to  $S_\infty^2$ . Then by referring to the fact that  $h_{\pi/2}$  is a homeomorphism, we will establish the stable cellularity of  $h_t$  to conclude the claim.

For each internal face  $\tau_i$ , a neighborhood of  $h_0(\tau_i)$  in  $h_0(\partial\sigma)$  is contained in one side of  $\mathbf{H}^3$  separated by  $H_i$ . We call the other side of  $H_i$  outwards. The outside of  $S_j$ 's is similarly defined using the image of external faces. Let  $H_i^t$  be the equidistant surface outside of  $H_i$  with the distance  $\int_0^t \sec \theta d\theta$ . This is not a geodesic plane but is a surface which intersects  $H_i = H_i^0$  at  $S_\infty^2$  with dihedral angle  $t$ . It can be seen also as an intersection of an euclidean metric sphere with the Poincaré disk meeting the unit sphere  $S_\infty^2$  with dihedral angle  $t$ . The angle  $t$  varies from 0 to  $\pi/2$ . As  $t$  increases,  $H_i^t$  is gradually pushed out towards  $S_\infty^2$ .

To define the image of an internal face  $\tau_0 = \tau$ , let us rearrange  $\tau_i$ 's in such a way that  $\partial\tau$  passes through  $h_0(\tau_1), S_1, h_0(\tau_2), S_2, \dots, h_0(\tau_k)$  and  $S_k$  in cyclic order.  $h_0(\tau)$  and  $h_0(\tau_i)$  meet on the intersection of  $H_0^0 = H^0$  and  $H_i^0$ . Take two internal faces  $h_0(\tau)$  and  $h_0(\tau_{i_0})$  having a common internal edge, and identify the edge with a segment on the  $z$ -axis in the upper half space model so that it meets  $S_{i_0}$  at the bottom end. See Figure 5 which shows the situation locally.  $H_{i_0}^0$  is a geodesic plane

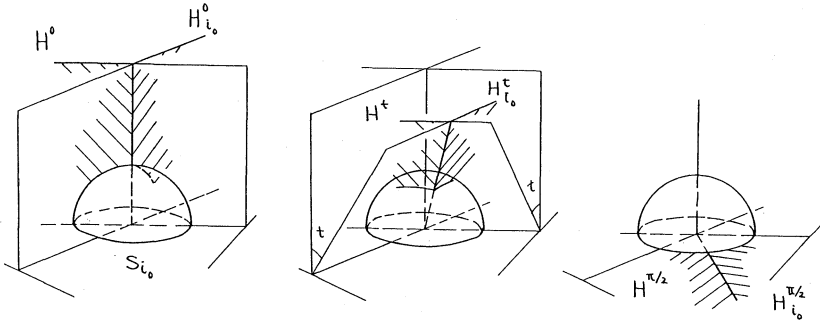


Fig. 5.

containing  $h_0(\tau_{i_0})$ .  $H_0^t$  and  $H_{i_0}^t$  are described in the second picture. In this coordinate, they are euclidean hyperplanes through the origin.

The original  $h_0(\tau)$  is a convex polygon on  $H^0$  bounded by the intersections with  $H_i^0$ 's and  $S_j$ 's where  $i, j = 1, \dots, k$ . As  $t$  increases, this region is gradually slid to again a convex region on  $H^t$  bounded by the intersections with  $H_i^t$ 's and  $S_j$ 's, and eventually reaches to a circular polygon on  $S_\infty^2$ . This bounded region on each  $H^t$  is the image of  $\tau$  by  $h_t$ . We have not ruled out the possibility that  $H^t$  intersects  $S_j$  for some  $j > k$ , but it will turn out that this never happen.

We next describe how to map the external faces. The trace of the deformation of  $H_i^t$ 's on the external boundary  $S_{i_0}$  viewed from the above is described in Figure 6. The image of an external face on  $S_{i_0}$  by  $h_t$  is a convex region on  $S_{i_0}$  bounded by the intersections with  $H_i^t$ 's. As  $t$  increases, the region is getting enlarged keeping convexity and finally fills up  $S_{i_0}$ .

$h_t$  is obviously a continuous deformation for  $0 \leq t < \pi/2$ , and is still continuous at  $t = \pi/2$  if we topologize  $\mathbf{H}^3 \cup S_\infty^2$  as a 3-ball. What is saved in this deformation is the property that  $h_t$  is an embedding on the set of external faces or on each internal face.

Modify  $h_{\pi/2}$  a bit to  $\hat{h}_{\pi/2} : \partial\sigma \rightarrow S_\infty^2$  by pushing each  $S_j$  outward to the disk on  $S_\infty^2$  bounded by  $\partial S_j$ . We claim that  $\hat{h}_{\pi/2}$  and hence  $h_{\pi/2}$ , and moreover  $h_t$  with  $t$  near  $\pi/2$  is a homeomorphism.  $\hat{h}_{\pi/2}$  is a local homeomorphism on the interior of each faces of  $\partial\sigma$  by the definition. It is also a local homeomorphism around edges and around vertices by the definition of  $h_t$  (see Figures 5, 6). Hence it is a local homeomorphism to  $S_\infty^2$ . Since  $\partial\sigma$  is compact and the image is simply connected, it must be

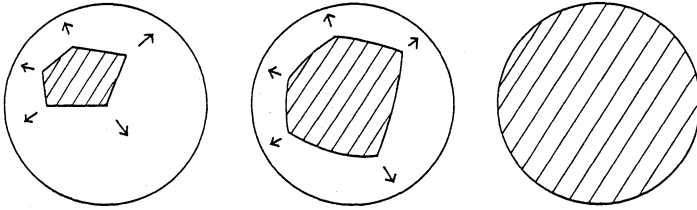


Fig. 6.

a homeomorphism.  $h_{\pi/2}$  is not quite different from  $\widehat{h}_{\pi/2}$  and is clearly a homeomorphism since so is  $\widehat{h}_{\pi/2}$ . The bent of the image by  $h_t$  is mild for  $t$  near  $\pi/2$ , and therefore,  $h_t$  is also necessarily to be a homeomorphism up to some moment.

For any  $0 \leq t < \pi/2$ , each  $H_i^t$  separates  $\mathbf{H}^3$  into a convex inward region and its complementary outward region. The intersections of any two of  $H_i^t$ 's look quite simple and are classified by the intersection of their boundaries on  $S_\infty^2$ . If the intersection on  $S_\infty^2$  is nonempty and transversal, then surfaces intersect transversely for all  $t$ . If the intersection on  $S_\infty^2$  is empty, then as  $t$  decreases, the intersection of surfaces is gradually changed from a circle, a point of contact to an empty set. It may be empty from the beginning. If the boundaries of surfaces on  $S_\infty^2$  are the same, then the intersection is empty for  $0 < t < \pi/2$  unless they are the same surface. The transversality of the intersections of  $H_i^t$ 's is missed only when either different surfaces without intersections for  $t > 0$  coincide at  $t = 0$ , or surfaces with circular intersection at the beginning contact at some moment.

We thus have a family of very visible stratifications of  $\mathbf{H}^3$  defined by the intersections of  $H_i^t$ 's and  $S_j$ 's. The intersection of their convex inward regions in  $\mathbf{H}^3$  is a compact convex stratum. The convex stratum bounded by  $H_i^t$ 's and  $S_j$ 's is certainly nonempty for  $t$  near  $\pi/2$ . On the other hand, by the continuity of the deformation,  $h_t(\partial\sigma)$  bounds a locally convex and hence a convex region in  $\mathbf{H}^3$  also for  $t$  near  $\pi/2$ . It is the same as the stratum bounded by  $H_i^t$ 's and  $S_j$ 's because of its convexity. Hence  $h_t$  is a cellular map  $:\partial\sigma \rightarrow h_t(\partial\sigma)$  with respect to the stratification of  $\mathbf{H}^3$  for  $t$  close enough to  $\pi/2$ .

In this stratification, every surface, that is any one of  $H_i^t$ 's and  $S_j$ 's, plays a role to determine a face of the convex stratum for  $t$  near  $\pi/2$ . A consequence to this stable property is that the map  $h_t$  is cellular with respect to the stratification of  $\mathbf{H}^3$  on an open interval in  $[0, \pi/2]$  including  $\pi/2$ . It also concludes that  $H_i^t$ 's are different each other for all  $0 < t < \pi/2$ .

As  $t$  decreases from  $\pi/2$ , this compact convex stratum is continuously compressed. If the stratum does not degenerate and the structure of the stratification on the boundary is kept in the deformation up to  $t = 0$ , then we are done since  $h_0$  turns out to be an embedding and the image bounds a convex polyhedron.

Otherwise, there is the first moment  $t_0 \geq 0$  at which  $h_t$  fails to be cellular since the cellularity is open. Then by continuity of  $h_t$ ,  $h_{t_0}(\partial\sigma)$  either still bounds a convex region, which is the convex stratum bounded by  $H_i^{t_0}$ 's and  $S_j$ 's, or degenerates to a convex set on some geodesic plane in  $\mathbf{H}^3$ . In the first case, the surfaces still in fact intersect transversely at  $t_0$ , but some edge of the stratification on the boundary of the convex stratum degenerates. Then two vertices must be close each other if  $t$  is near  $t_0$ . However the vertices of the stratification on  $h_t(\partial\sigma)$  for  $t > t_0$  is the image of the vertices of  $\partial\sigma$  by the definition of  $t_0$ , and hence their mutual distance is bounded away from zero by the definition of  $h_t$ . This is contradiction. In the second case, the faces of  $\partial\sigma$  are mapped on the same geodesic plane by  $h_{t_0}$ . Hence three vectors from a vertex of  $\partial\sigma$  to adjacent vertices in the image of  $h_{t_0}$  must be linearly dependent. However they are always independent by the definition of  $h_t$ . This is also a contradiction. Q.E.D.

*Proof of Proposition 5.2 and Theorem.* Assigning to each block of  $\tilde{K}$  a polyhedron bounded by the image of its boundary, we get a map from  $\tilde{K}$  extending  $h : \tilde{K}^{(2)} \rightarrow \tilde{\Delta}^{(2)}$ . It is a local homeomorphism on the interior of blocks. We have already seen that it is a homeomorphism on the boundary. Hence it is a local homeomorphism everywhere since there is no vertices in the interior and every cell meets the boundary. The surjectivity is obvious. Since the image is simply connected, it must be a homeomorphism.

$\tilde{\Delta}^{(2)}$  now determines a convex polyhedral decomposition  $\tilde{\Delta}$  of  $N$ . The decomposition is invariant under the action of  $\pi_1(N)$  and the map can be chosen to be equivariant. Hence it determines a convex polyhedral decomposition  $\Delta$  on  $N$  with a descending equivalence from  $K$  to  $\Delta$ .

Q.E.D.

**References**

- [ 1 ] Epstein, D. B. A. and Penner, R., Euclidean decomposition of noncompact hyperbolic manifolds, *J. Differential Geom.*, **27** (1988), 67–80.
- [ 2 ] Kojima, S. and Miyamoto, Y., The smallest hyperbolic 3-manifolds with totally geodesic boundary, *J. Differential Geom.*, **34** (1991), 175–192.
- [ 3 ] Kojima, S., Polyhedral decomposition of hyperbolic manifolds with boundary, preprint, Tokyo Inst. Tech. (1991).
- [ 4 ] Thurston, W. P., “The Geometry and Topology of 3-Manifolds”, Lecture Note, Princeton University, 1977.

*Department of Information Science  
Tokyo Institute of Technology  
Tokyo 152  
Japan*